Chapter 10

Using Magnetic Resonance Imaging in the Early Detection of Alzheimer's Disease

Emily J. Mason, Manus J. Donahue and Brandon A. Ally

Additional information is available at the end of the chapter

http://dx.doi.org/10.5772/54445

1. Introduction

Alzheimer's disease (AD) is the most common form of dementia. While many strides have been made in elucidating the underlying causes of AD, studying the disorder *in vivo* has faced several hurdles: First, the structures affected by AD lie deep within the brain where biopsy is not practical. Second, animal models do not develop AD naturally, and genetically engineered models designed to mimic AD do not fully reproduce the human phenotypes [1-3]. Third, while studies using Positron Emission Tomography (PET) have been very useful for examining plaques and metabolic changes, they involve the injection of radioactive contrast agents. Many of these materials have short half-lives and must be created on-site, making PET very expensive and difficult to be performed at non-specialized centers. Finally, studies which examine cerebrospinal fluid (CSF) require participants to undergo an invasive and sometimes painful lumbar puncture, potentially on multiple occasions [4-7]

In contrast to other techniques, Magnetic Resonance (MR) offers a non-invasive method for analyzing structural and functional brain characteristics without the need for ionizing radiation. In other words, it can be performed in longitudinal studies without significant health concerns. Multiple scans can be performed quickly in the same testing session to assess tissue response to tasks or pharmacological administration. The scans are generally 2-5 minutes each and many analyses can be done post-hoc. Conveniently, most hospitals and clinics already possess the MR scanners at field strengths of 1.5 and 3.0 Tesla (T).

Many MR techniques have been used to understand the underlying pathology in patient populations already diagnosed with AD. Because MR studies require absolute stillness for several minutes, and some functional scans require the patient to focus on perform-

ing a difficult task, performing MR work in advanced AD cases is quite challenging and as such, most studies are limited to mild and very mild cases. While these studies are typically performed at a time when pathology is irreversible, the results of this work point to changes that may be apparent before cognitive decline has become clinically apparent. For this reason, studies that examine differences between people who will eventually develop AD and people who will not develop AD provide insight into both the cause and the physiology of the disease.

It is impossible to predict with certainty who will develop AD, but there are several factors that increase the risk. These at-risk populations include individuals in the prodromal stage of AD, termed amnestic mild cognitive impairment (aMCI), and people at a genetic risk for developing AD. A diagnosis of aMCI indicates that there is more memory decline than would be expected based on the person's age and education level, however memory impairment is not interfering with daily activities. It is estimated that 10-20% of people 65 and older have aMCI, and out of those 10-15% will progress to develop AD in 3-4 years. [8,9] Because approximately 30% of people diagnosed with aMCI will remain stable or improve over time, it is important to find biomarkers that will identify those most likely to progress to AD.

This chapter will focus on the use of MR in the early detection of AD. Major advances have been made in structural imaging of both gray and white matter using proton density, T1- and T2- weighted imaging, and Diffusion Tensor Imaging (DTI). Functional imaging in AD will also be reviewed, and Blood Oxygenation Level-Dependent (BOLD) functional Magnetic Resonance Imaging (fMRI) will be broken down into its primary contributors: Cerebral Blood Flow (CBF), Cerebral Blood Volume (CBV), and the Cerebral Metabolic Rate of Oxygen ($CMRO_2$). Finally, hemodynamic fMRI contrast can be complemented using measures of neurochemistry, including measuring the balance between excitatory (glutamatergic) and inhibitory (γ-aminobutyric acid; GABAergic) neurotransmission. This can be achieved with new single-voxel chemical imaging techniques such as Magnetic Resonance Spectroscopy (MRS), or more recently using multi-voxel MRS imaging (MRSi)

2. Basics of MRI

Before reviewing the work that has been done with MR, a brief overview of the theory behind MR should be covered. MR physics can essentially be understood using principles of classical physics, however for a more comprehensive understanding the reader is directed to an excellent review by Plewes and Kucharzck [4,10]. Briefly, MR takes advantage of the behavior of a system of protons in the presence of a magnetic field and how this behavior changes based on the micro- and macroscopic environment. Magnetic strength is generally reported in units of Tesla (T), and MRI scanners have very high field strengths. In human research, 1.5T, 3T, and 7T scanners are commonly used, though 1.5T and 3T scanners predominate the clinical setting. The magnet's strength and direction is represented by the vector B0 (see Figure 1), and lies along the Z-axis (generally from foot to head).

http://dx.doi.org/10.5772/54445

Due to the large amount of water that constitutes tissue (~80-99% depending on tissue type), most MR is specifically focused on the protons on water molecules. Protons have an intrinsic spin that in nature is oriented randomly. In the presence of a magnetic field however, these spins align themselves on average parallel or antiparallel to the axis of the field (Figure 1a). The number of protons aligned parallel to the field is very slightly larger than the number of protons aligned antiparallel, and it is this difference that produces the net magnetization vector in a voxel. When a radiofrequency (RF) pulse is applied at the proper frequency (Larmor frequency), the longitudinal (z) component of the magnetization vector is tipped away from the axis of the main magnetic field, but continues to spin around the longitudinal axis or "precess" (Figure 1b). When the pulse is removed, the longitudinal component of the magnetization vector will realign itself with the field with a unique time constant that varies with the local environment.

Manipulating the timing of the RF pulses controls the magnetization and creates the desired contrast. The most fundamental timing parameters of relevance are repetition time (TR), echo time (TE), and in some cases inversion time (TI). TR is the time between consecutive acquisitions, and TE is the time from the onset of the excitation pulse that is used for preparing the signal for detection to the signal refocusing and in most cases acquisition. In an inversion recovery pulse sequence, TI refers to the time between the inversion pulse and the excitation pulse. Importantly, simply by manipulating the timing of the above parameters a range of MR contrasts can be obtained with varying sensitivity to different tissue types. A simple pulse sequence indicating RF and gradient timing is illustrated in Figure 1c.

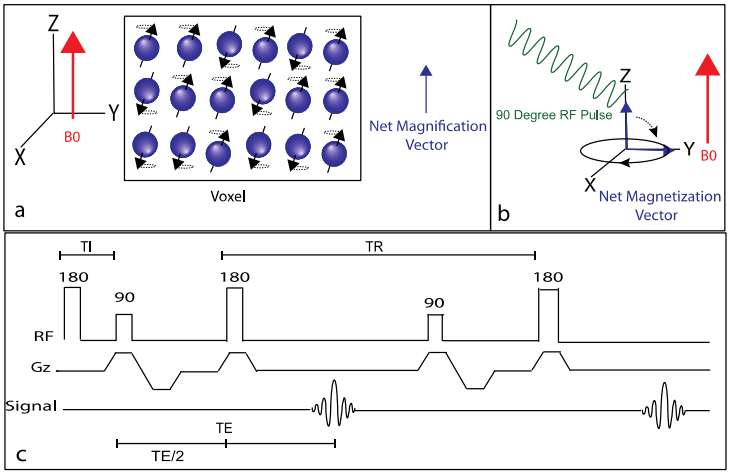

Figure 1. Physics underlying magnetic resonance. Hydrogen atoms align parallel and antiparallel to a strong magnetic field, producing a net magnification vector (a). When a radio frequency pulse is applied at the Larmor frequency, the net magnetization vector is tipped away from the main magnetic field (b). Example of a simple pulse sequence showing timing parameters of the application of radio frequency pulse (RF), the onset of gradients in the Z direction (Gz), and the timing of signal acquisition (Signal) (c).

In most cases, the detectible signal (S) that is measured in MRI is a combination of three primary factors: water proton density (C; ml tissue /100 ml water), magnetization in the longitudinal plane (M_Z) and magnetization in the transverse plane (M_{XY}):

$$S \propto C \bullet M_Z \bullet M_{XY} \tag{1}$$

The two major methods or "weighting" that are used for generating contrast are T1 and T2. T1 and T2 are independent measures and reflect different properties of the tissue of interest, with T1 governing the M_z term and T2 the M_{xy} term in Eq. 1 above. The time it takes for the magnetization to realign itself longitudinally is measured using T1 weighting (Figure 2a), and is achieved with a short TR and a short TE sequence. T1 is a constant that is unique for each tissue type and is equal to the point when 63% of longitudinal magnetization is recovered (Figure 2b). At the times selected for T1 imaging, there is a high amount of contrast between gray and white matter and therefore T1 weighted imaging is useful for viewing structural changes in the brain (Figure 2c).

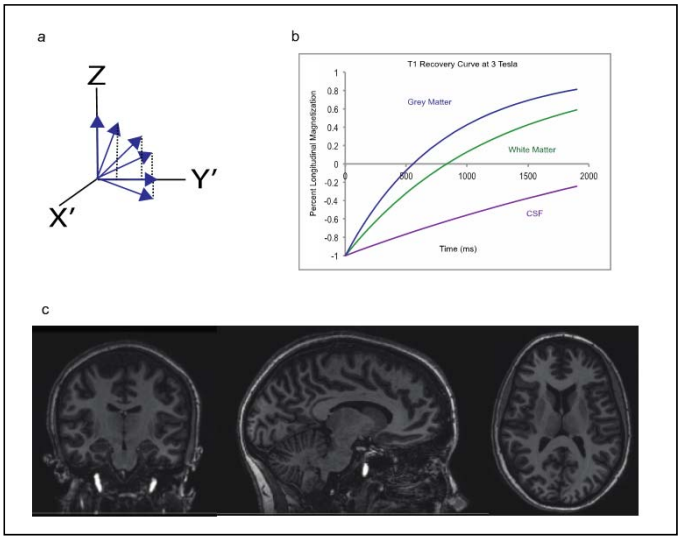

Figure 2. T1 weighted imaging. After removal of an RF pulse the magnetization vector recovers longitudinally (a). The recovery time is a constant for each tissue type based on the magnetic field strength that is applied (b). Example T1 weighted images (c).

The M_Z component of the magnetization vector is based on pulse timing as well as the T1 of tissue, and for magnetization following a pre-pulse with flip angle, α, is given by:

$$M_Z = \left(1 - \alpha e^{\frac{-TI}{T1}} + e^{\frac{-TR}{T1}}\right) \tag{2}$$

http://dx.doi.org/10.5772/54445

Note that in the absence of a prepulse (α=0), the TR determines the T1-weighting. When the RF pulse is applied, individual protons will also precess in synchrony in the transverse plane. When the pulse is removed, the protons will lose that synchrony or dephase, which results in a reduced M_{XY} (Figure 3a). This is referred to as T2 decay. Like T1, the T2 time constant is unique for each tissue (Figure 3b). Unlike T1, T2 weighting is achieved with a long TE and long TR.

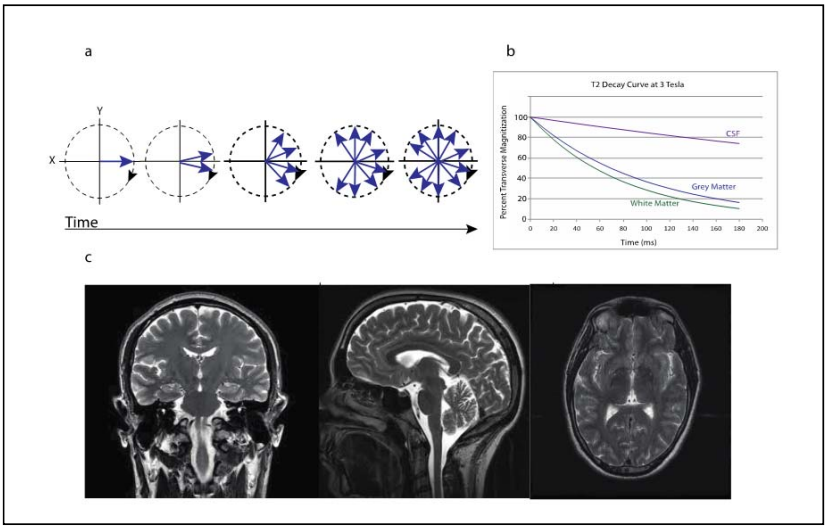

Figure 3. T2 weighted imaging. Protons lose synchrony after removal of an RF pulse (a). The amount of time it takes for protons to lose synchrony is a constant that is unique to each tissue type (b). Example of T2 weighted images (c).

The M_{XY} component of MRI is based on pulse timing as well as the T2 constant of the tissue area, and can be written:

$$M_{XY} = e^{-TE/T2} \tag{3}$$

The three equations can be combined to form one overall equation for the MR signal that takes into account both the T1 and the T2 properties of the tissue:

$$S \propto C \bullet \left(1 - \alpha e^{\frac{-TI}{T1}} + e^{\frac{-TR}{T1}}\right) \bullet e^{-TE/T2} \tag{4}$$

T1 and T2 components are each present whenever a proton is flipped out of alignment, but by manipulating the pulse sequences one can contribute to the signal more than the other. This is referred to as weighting. If neither the T1 nor the T2 signal contributes strongly to the signal, only the C component is left. These images are referred to as proton density images.

3. Structural imaging

By far, the most established use of MR is to examine the gross anatomy of the brain. With the right specifications, MR can provide a highly detailed three-dimensional image that allows for the examination of brain structures. Weighting is used to provide contrast for the tissue of interest.

3.1. Anatomical imaging

T1 weighted imaging is used to visualize structural changes in tissue. At a field strength of 3 Tesla, T1 weighted images can be acquired in about five minutes and have a resolution of approximately 1 mm^3.

The most significant differences reported in patients are atrophy of the structures in the medial temporal lobe (MTL) which typically follow the "Braak stages" of AD progression [11]. Briefly, pathology starts in the transentorhinal region (stages I and II), moves to the limbic region (stages III and IV) and ends in isocortical regions (stages V and VI). Studies that have been done in AD patients show that hippocampal and entorhinal cortex volume change, as well as temporal lobe morphology changes are the best measures to predict change over time [12]. A higher level of regional brain atrophy has also been associated with decreased levels of Aβ-42 and increased levels of phosphorylated tau in the CSF of AD patients [12].

In patients who have been diagnosed with aMCI, changes to the parahippocampal region are already apparent. It is up for debate whether the investigation of the entire brain or just volumes of interest (VOIs) are better at predicting conversion from aMCI to AD, but in a recent meta-analysis of work using data from the Alzheimer's Disease Neuroimaging Initiative (ADNI) only four methods were able to distinguish those who would convert more accurately than random chance. None of the four were more statistically reliable than the others, but three examined VOIs (Voxel-STAND, 57% sensitivity and 78% specificity; Voxel-COMPARE, 62% sensitivity and 67% specificity; Hippo-Volume, 62% sensitivity and 69% specificity) while only one examined the entire brain (Thickness-Direct, 32% sensitivity and 91% specificity) [11,13-15]. A protocol devised by Chincarini et al. to sample several VOIs has demonstrated a method of separating converters from non-converters with a sensitivity of 71% and a specificity of 65% [16,17]. Another method for predicting conversion is examining hippocampal shape, and Costafreda et. al. were able to develop a method with 77% sensitivity and 80% specificity. [18,19].

Patients that are at-risk for AD but have no cognitive deficit are much more difficult to identify. Most studies have been done in carriers of the ApoE ε4 allele, however it is important to remember that these studies have been cross sectional, and therefore may reflect a consequence of the gene that makes carriers more susceptible to AD, but not necessarily a stage of AD itself. There have been cortical thinning signatures identified in children, adolescent, and young adult carriers of the ε4 allele. These signatures reflect reductions in dorsolateral and medial prefrontal, lateral, temporal, and parietal cortices. [20-22]. Middle-aged carriers

http://dx.doi.org/10.5772/54445

of the ε4 allele were found to have a thinning of the cortex in the entorhinal region, subiculum, and other MTL structures, although the results were stronger in those with a family history of AD than those that carried the ε4 allele alone [23,24].

The detectible changes are not limited to atrophy. There have been several studies that have discovered an increase in gray matter in young adult carriers of the ε4 ellele. Increases were found in bilateral cerebellar, occipital, and thalamic regions as well as in the fusiform and right lingual gyri [22,25]. Recent work has also suggested that changes in the basal cholinergic forebrain may be detectible decades before cognitive impairment, although this study did not take into account genetic status [26].

One of the significant weaknesses of analyzing structural changes is that the regions of interest can vary in size even across healthy individuals. Longitudinal studies are the only way to control for this variability. Secondly, the atrophy of brain regions likely occurs secondary to functional changes. The assessment of atrophy alone gives little information as to the underlying factors that led to neuronal loss.

3.2. White matter imaging

Unlike T1 weighted imaging, T2 imaging relies on the dephasing of the magnetization vector in the transverse plane. T2 weighting, specifically FLuid Attenuated Inversion Recovery (FLAIR) imaging, is used to identify White Matter Hyperintensities (WMH), which are increased in AD [27]. In contrast, diffusion tensor imaging (DTI) is able to indirectly measure the integrity of myelin sheaths surrounding white matter tracts, and Susceptibility weighted imaging (SWI) is able to distinguish tissues at a high resolution based on several properties.
FLuid Attenuated Inversion Recovery (FLAIR) and Diffusion Tensor Imaging (DTI)

If simply T2 weighted imaging was used, the signal from Cerebrospinal Fluid (CSF) is strong and therefore very bright (T2 of CSF ~ 600 ms at 3T). This makes it difficult to see subtle abnormalities in the white matter regions that partial volume with CSF. FLAIR imaging nulls the signal from CSF so that the image is focused solely on the white matter. The first RF pulse inverts the magnetization by 180 degrees. Then, when the longitudinal magnetization for the CSF = 0, an excitation pulse and readout is applied. Because T1 of CSF (~4000 ms at 3T) is much longer than that of tissue (T1~700-1200 ms at 3T), residual tissue signal remains at the time of the CSF nulling.

DTI measures fractional anisotropy (FA), a quantitative measure of the coordinated movement of water molecules. FA assumes that the stronger a white matter tract is, the more likely the water molecules will be to move along the tract rather than sideways within the myelin sheath. If the myelin sheath is damaged it becomes easier for water molecules to diffuse through it, and the FA value will decrease.

The loss of white matter integrity, either through WMH or FA differences, may correlate with increasing cognitive impairment [28,29]. In AD populations reduced FA values have been found in frontal and temporal lobes, the posterior cingulum, the corpus callosum, the superior longitudinal fasciculus and the uncinate fasciculus [30]. Both WMH and FA have been found to distinguish normal aging from aMCI[31] and predict conversion from aMCI

to AD[32]. Results have differed in whether they correlate with ApoE ε4 status, with some studies saying they do not [33,34], while several others say they do [35-37]. Note that the studies that claim white matter integrity correlates with ApoE ε4 status are more recent, and their ability to detect differences are likely more sensitive. White matter integrity has also been found to correlate with a family history of AD regardless of ApoE status [38,39].

White matter hyperintensities are associated with vascular abnormalities and therefore highly correlated with cardiovascular disease. For this reason, many clinicians will exclude a diagnosis of AD if there are many apparent WMH and instead diagnose the patient with vascular dementia [32]. Many non-amnestic MCI patients tend to have a higher degree of cardiovascular disease than those with aMCI or AD, however aMCI and AD patients have increased WMH scores. For this reason, increased WMH scores in cognitively impaired individuals is likely associated with neurological disease rather than vascular disease [32].

Susceptibility Weighted Imaging (SWI)

Susceptibility weighted imaging is a method that can discriminate tissue content with a high level of resolution based on the tissue's intrinsic magnetic properties. SWI uses T2* weighting along with magnitude and phase information to enhance contrast, and when combined with traditional MR weighting it can be used to detect small differences in susceptibility between blood and tissue. It is particularly useful for detecting cerebral microbleeds because it can exploit the magnetic properties of blood since the susceptibility effects from fully oxygenated (arterial) and partially de-oxygenated (venous) blood water, and tissue, varies greatly – especially at high field strength. It can also be used to measure the iron content of a tissue.

Microbleeds are inversely correlated with performance during cognitive testing in healthy older adults, although this finding has never reached significance in an AD population [13,14]. SWI would allow for improved visualization of microbleeds so that if there is a relationship between microbleeds and susceptibility to AD pathology, it can be recognized. Techniques are being developed that semi-automatically detect cerebral microbleeds with little human interference. These would significantly reduce the processing time and standardize the quantification of microbleeds across patients and imaging centers.

In addition to microbleeds, one marker of oxidative stress is an increase in a tissue's iron content. Iron levels are highly elevated in AD patients as well as those with aMCI, and it is thought that changes in iron content may be detectible decades before the onset of the disease [16]. There is a theory that Aβ deposition may occur as a cellular response to an increased level of iron, and this is one of the underlying causes of amyloid plaque formation[40]. SWI has been shown to be a promising method to non-invasively assess iron distribution, and determine if there is a link between iron accumulation and the onset of AD pathology [18].

SWI has only been used as a technique since 2004, which makes it very new technology. Although it has not yet been used in an at-risk population, SWI studies will likely be important tools in assessing AD risk.

http://dx.doi.org/10.5772/54445

3.3. Future of structural imaging

There is still a lot of work to be done in structural imaging. Most clinical studies to date have used 1.5 Tesla (T) scanners, however many medical centers now have 3T scanners and there are approximately 50 7T scanners worldwide. These high-field scanners allow for increased resolution, and provide better spatial resolution for observing structural changes in the same scan time. Although 7T scanners are not yet FDA approved for clinical use, they are already being utilized in neuroimaging research, including in patients with AD.

Many atrophy measurements are made either through a trained radiologist's visual assessment, or by manually tracing the area of interest. As such, the measurement of atrophy can be subjective, and is not always reproducible across testing site. In fact, one study found that the ability of radiologists to diagnose subjects based on atrophy alone had a specificity of 85% and a sensitivity of only 27% [20]. The introduction of FDA-approved methods that can automatically detect atrophy will create standardization of the field, and decrease variability across medical centers [41].

4. Functional imaging

While structural imaging is important to assess brain atrophy, the hope is that AD pathology will be identified before neuronal death so that atrophy can be prevented. One current theory is that one of the major components leading to amyloid and tau pathologies could be vascular changes [42]. Two of the risk factors for AD are mutated forms of APP, and the ApoE ε4 isoform and both of these factors are involved in cholesterol processing. The inability of a neuron to clear amyloid plaques may be prognostic and indicate impaired blood flow as a risk factor for AD. While it is not immediately apparent how blood flow is contributing to AD, some vascular changes are being evaluated through the use of hemodynamic-based functional imaging techniques.

4.1. BOLD fMRI

Functional magnetic resonance imaging, or fMRI is a way to gain insight into the functional processes occurring in the brain. Most fMRI modalities are based on the blood oxygenation level-dependent (BOLD) effect. This is an indirect method of tracking the activation or inactivation of brain regions relative to a baseline state, and is based on the idea that an active area will need more energy and consume more glucose and oxygen and therefore more blood will need to be directed to that area. More specifically, oxygenated and deoxygenated blood water have different intrinsic magnetic properties (oxygenated blood is diamagnetic and deoxygenated blood is paramagnetic) and therefore affect the T2 and T2* relaxation times of surrounding water in blood and tissue in different ways. Deoxygenated blood has a strong enough magnetic affect (paramagnetic) that it will distort the local field and decrease the signal intensity (i.e. shorten T2) of surrounding water for that region. Oxygenated blood will not have the same effect, and therefore regions containing more oxygenated blood will have higher signal intensity (longer T2). Importantly, during functional activation the cere-

bral blood flow increases by a large amount (20-100%) relative to the cerebral metabolic rate of oxygen consumption (CMRO2), resulting in a relative decrease in the concentration of deoxyhemoglobin in capillaries and veins. By comparing the signal intensities of regions at baseline (Figure 4a) and during a task (Figure 4b), the regions that have an increase in capillary and venous oxygenation can be visualized.

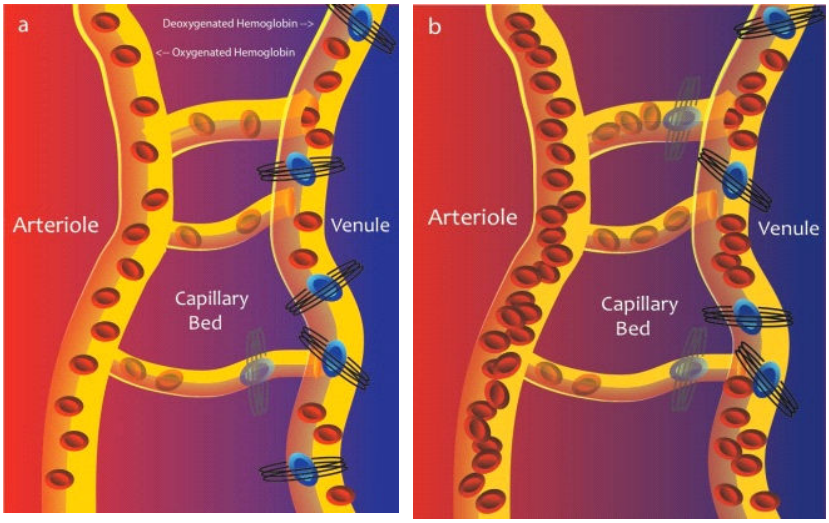

Figure 4. Blood flow at rest (a) and during activation (b)

BOLD imaging involves very fast sequences in order to visualize changes in functional activation on the timescale of the hemodynamic response. This rapid sequencing allows for a time resolution of approximately 2s. Total time required to perform a BOLD scan varies with the task being performed, but typically scans take 5-15 minutes.

There are two main types of fMRI: evoked (task-related) and spontaneous ("resting" state). Evoked fMRI is the more commonly performed test in which the same task is repeated many times with a baseline measurement taken between trials. Statistical tests (Z- and t-tests) are used to differentiate the regions activated during the task from those active at baseline. By contrast, spontaneous BOLD specifically measures synchrony of baseline signal fluctuations to determine how the brain is functionally connected.

http://dx.doi.org/10.5772/54445

Evoked BOLD fMRI

There are several established testing paradigms that have been designed to study memory. The most commonly used paradigms look specifically at either episodic or semantic memory. Episodic memories involve the recognition of autobiographical or cued information (e.g., faces, words, other visual stimuli) while semantic memory involves the recognition of a fact or information regardless of personal context (e.g., famous faces, geographical locations). Because episodic memory is highly affected by AD, many fMRI paradigms use an episodic memory task to elicit functional differences between patients and controls. While encoding a new memory, activation of the hippocampal and parahippocampal regions is decreased in mild AD patients compared to healthy controls [43]. In a block design face name paradigm, AD patients also show decreased hippocampal activation to novel stimuli compared to repeated comparisons [43].

A multitude of studies have been performed in asymptomatic carriers of ApoE ε4 with mixed results. In an extensive review of the literature by Trachtenberg et al, some claim that carriers have increased activation across brain structures while others claim the opposite[44]. Moreover, there have been reports of both increases and decreases of activation or that there is no significant effect at all of carrying the ApoE ε4 allele[44]. In each case, investigators have provided hypotheses to explain both increased and decreased activation in ApoE ε4 carriers: decreased activation can be easily explained by the fact that presymptomatic carriers are already accumulating AD pathology hallmarks before cognitive decline is experienced. These pathologies may be hindering the BOLD response in the specific areas that experience a decrease in activation, or they may be inhibiting areas that lie functionally upstream. In contrast, an increase in activation can be explained in two ways, which take into account AD pathology. For one, the accumulation of pathology may lead to the dedifferentiation of neural network such that many networks become involved in a specific process. This may in fact be a part of healthy aging [45] and could be found in young, presymptomatic carriers of ApoE ε4 because their brains are aging more rapidly. Alternatively, the brain may have a cognitive reserve that needs to "work harder" during a difficult task to perform at a normal level, and thus would have a higher amount of activation. Trachtenberg et al [44] argue that the populations tested in these studies are very young (20s and 30s) and have a great deal of time before they will begin to experience cognitive decline. He suggests instead that the possession of an ApoE ε4 allele leads to a fundamental difference in neurophysiology that could be contributing to this effect.

A growing body of evidence suggests that an episodic memory task may not be the best way to characterize memory loss because episodic memory declines as a part of healthy aging as well. Episodic memory tasks are also more difficult than semantic memory tasks, The work may therefore be experiencing a basement effect[45]. Semantic memory, in contrast, is affected very early in AD, but remains relatively untouched in the healthy aging process [45]. Most semantic memory tests involve the recognition of famous names and faces [45-47] or categorizing word lists [1,3]. These types of studies have shown an increase in activation and a decrease in deactivation the MTL regions of carriers of the ApoE ε4 allele.

Spontaneous BOLD fMRI

Resting state, or functional connectivity MRI (fcMRI) is a task-independent measurement of brain regions that fluctuate in their BOLD signal together, indicating that they are functionally connected. The Default Mode Network (DMN) is a collection of brain regions that seem to activate together while the brain is at rest, and are deactivated while the brain is engaged in a cognitive task. The DMN is composed of MTL and lateral frontal regions, particularly the posterior cingulate complex [4,6,7]. This network is altered in AD and is a potent biomarker for separating patients with AD from healthy controls [8], patients with aMCI from healthy controls [48], and genetically at-risk individuals from healthy controls [4].

Caveats to BOLD fMRI

Although BOLD fMRI is an important tool for research, there are some limitations to its clinical feasibility as a biomarker for future AD. To date, it has not successfully been used in predicting patient prognosis or trajectory. In terms of practicality, fMRI is expensive and requires extensive image processing, which will drive up the cost of any tests. It is also not completely reproducible across testing sites or days. Different equipment and software can create variables in data analysis across testing sites. Longitudinal studies can present difficulties because as they age, patients may develop comorbidities, or begin taking drugs that will interfere with the BOLD signal in a way unrelated to AD pathology. Even subtle changes can influence the BOLD signal such as recent alcohol [49] or caffeine [50] intake.

The biggest difficulty with BOLD fMRI is that it is generally not quantitative. Changes in blood oxygenation are based on three individual components: Cerebral Blood Flow (CBF), Cerebral Blood Volume (CBV), and the Cerebral Metabolic Rate of Oxygen ($CMRO_2$) [51]. Figure 5 represents the many ways that CBF, CBV, and $CMRO_2$ can contribute to the BOLD effect. It is impossible to determine which of these is contributing to a BOLD fluctuation with fMRI alone. For this reason, vascular imaging techniques are being developed that are able to quantitatively determine the physiological changes that are contributing to the BOLD signal. Techniques to quantify CBF and CBV have been validated and are gaining popularity. $CMRO_2$ methods are still in development and have not been used in an AD population and will therefore not be covered.

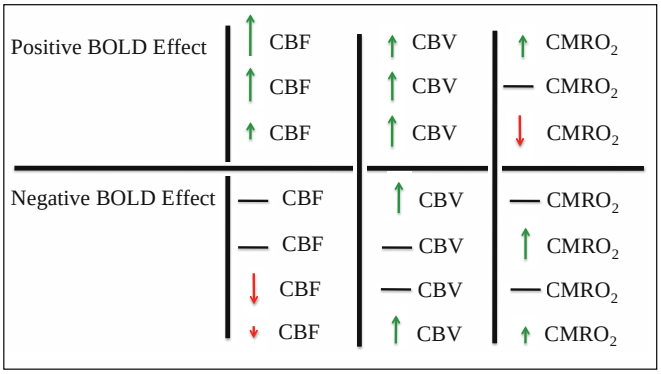

http://dx.doi.org/10.5772/54445

Figure 5. Positive and negative BOLD effects are influenced by CBF, CBV, and CMRO2 and it is not possible to distinguish which factor is contributing by only measuring BOLD.

4.2. Cerebral blood flow

Cerebral blood flow is a measurement of the rate of tissue perfusion, usually measured by the amount of blood that reaches a tissue per unit time (mL blood per 100 g tissue per minute) [52]. CBF has been quantified by Positron Emission Tomography (PET) [53,54] and Single Photon Emission Computed Tomography (SPECT) [10,55,56] but today it can also be quantified noninvasively using a technique called Arterial Spin Labeling (ASL). ASL uses a radiofrequency pulse to label blood water in an area outside of the region of interest, usually in the neck. After 1-2s, the labeled blood water flows into the imaging region and exchanges with tissue water and a tagged image can be obtained [51,57]. This image is compared with an image where the blood water is not labeled, and the difference between the two images provides a map proportional to CBF. As can be seen, ASL is analogous to tracer-based approaches such as 15O PET and Gadolinium-MRI, however the tracer is endogenous blood water as opposed to an exogenous contrast agents. Whole-brain ASL scans can be performed in less than 5 minutes with a spatial resolution of 3-5 mm.

In AD patients, deficits in CBF have been seen in the temporoparietal cortex, posterior cingulate cortex, and frontal cortex [57-59]. CBF as measured by ASL has been shown to be increased in aMCI patients but decreased pre-symptomatic carriers of ApoE ε4 [11,60]. The increase that is seen in aMCI has been attributed to compensatory mechanisms [60].

Often, changes in blood flow precede structural changes, but reduced CBF is not necessarily an indicator of vascular dysfunction. For instance, CBF alterations may be due to a lower metabolic demand, cardiac output, or blood pressure [10,61,62]. Longitudinal analysis of CBF in at-risk populations should be developed for its potential as a method for tracking disease progress or recognizing it before cognitive symptoms begin.

4.3. Cerebral blood volume

Cerebral blood volume measures the amount of blood per 100 mL brain tissue. It is an indirect measurement of the vascularization of brain regions, and is less dependent on the subject's respiration than CBF[11,15,63,64]. There are currently two major techniques that measure CBV: Dynamic Susceptibility Contrast MRI (DSC-MRI) and Vascular Space Occupancy MRI (VASO). DSC-MRI involves the injection of gadolinium as a contrast agent, and is the best validated measure. Unfortunately, the injection of gadolinium is dose-restricted because of its toxic effect on kidneys which limits its potential for longitudinal studies and older patient populations [17,65]. VASO is a completely non-invasive method of measuring CBV changes and has been gaining popularity in recent years. Unlike DSC-MRI, VASO uses endogenous blood water as a contrast agent. VASO can be performed by measuring the tissue signal with and without blood water nulled, and subtracting one image from the other. Although VASO is correlated with DSC-MRI there are some minor variations in the two measurements, suggesting that the underlying physiology may be different [19,63].

VASO has been applied to a mixed group of patients with aMCI and AD and found that there are CBV reductions in the frontal and parietal lobes. These reductions were most striking in white matter which suggests that any vascular component of AD is especially damaging to white matter compared to gray matter [21,22,61]. In the future, longitudinal studies should be performed in carriers of ApoE ε4 to determine if these white matter vascular deficiencies can be recognized at a young age.

5. Chemical imaging

Structural and functional imaging are important for assessing the damage caused by AD, but for designing therapeutics the ability to view changes at the macromolecular level would be highly beneficial. New techniques are being developed that can do just that. Magnetic Resonance Spectroscopy (MRS) can be done in a single voxel or across multiple voxels (MRS imaging, MRSi) to assess macromolecular concentration. Both are new techniques that are still being optimized, but will be extremely useful in understanding AD.

5.1. Magnetic resonance spectroscopy

MR imaging primarily measures signal from water protons, but in MR spectroscopy protons of various metabolites can be assessed at one time. Quantification is achieved by exciting a single voxel with a combination of RF pulses, and obtaining a free induction decay (FID) spectrum. When this spectrum is Fourier transformed, metabolites can be visualized due to their variability in chemical shift (Figure 6). Because the chemical shift of a single metabolite is constant, it will always peak at the same frequency (measured in parts per million, ppm). By calculating the area under the peak, the concentration of a metabolite relative to an internal standard can be obtained.

http://dx.doi.org/10.5772/54445

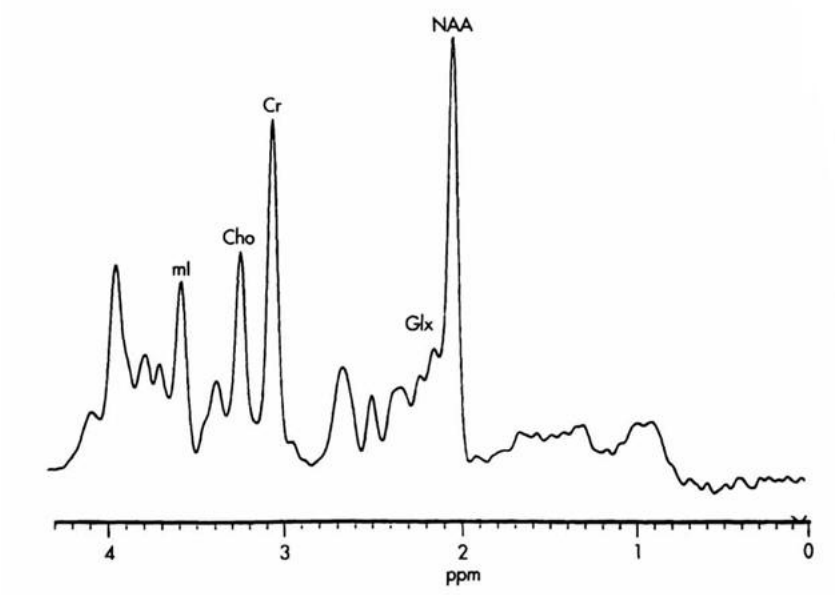

Figure 6. Example of chemical shift spectrum from a normal brain (from the University of Missouri-Kansas City Radiology Resident Resource Webpage

The most common macromolecules studied in neuroimaging are creatine (Cr) which is usually unaffected by disease and can act as an internal standard, *N*-acetyl-aspartate (NAA), a marker for neuronal health, myo-inositol (mI), a marker of gliosis [32,66], and choline (Cho). In AD, NAA is typically decreased in AD and mI is typically increased so NAA/Cr, mI/Cr and NAA/mI ratios are good markers of the disease with the ratio of NAA to mI being the strongest. The mI concentration has been found to be elevated in aMCI [33,34,67]. There is a trend that NAA is decreased in aMCI, however the effect is much more mild if it exists [35-37,68]. Glutamate (Glu) is the primary excitatory neurotransmitter, and is significantly reduced in AD [69] Gamma-amino butyric acid (GABA) is an inhibitory neurotransmitter, and its concentration may be decreased in AD [70]. It is possible to use MRS to estimate relative concentrations of both Glu and GABA *in vivo*, but due to their low concentrations compared to NAA and other metabolites, and the fact that signal from these metabolites is very close in frequency space to other metabolites of larger concentration, it is more difficult to identify them without suppressing or "editing" other signals. One of the common methods used to quantify GABA is a PRESS or MEGA-PRESS sequence which suppresses or edits signals from water, creatine, and other nearby metabolites so that the characteristic GABA peaks can be identified. For more information on the MEGA-PRESS sequence, see Waddell 2007 [71].

The importance of MRS research is clear, but there are some difficulties associated with it. To begin with, the scans take a long time to complete—more than ten minutes in

some cases—and because the measurements are taken in a single voxel the subject must stay absolutely still throughout the scan. This is very difficult for young healthy subjects, and may be nearly impossible in older, demented subjects. Common sedation drugs such as propofol will change the levels of brain metabolites and should be avoided[72]. In premenopausal women GABA levels also vary depending on the stage of the menstrual cycle, and may introduce variability[73].

Typically, spectroscopy is done in the posterior cingulate or medial temporal cortices, but these are only affected by AD in late stages of the disease. It would be more helpful to study the smaller limbic areas that are affected sooner, but the voxel sizes typically used in spectroscopy are larger than many of these areas [66]. Falini et al developed a technique to perform spectroscopy across the entire brain and found that NAA levels are reduced in those with AD, however whole-brain spectroscopy is a non-specific marker [41,74]. These limitations will be overcome with higher field strength, advances in shimming algorithms, and improvements to computerized registration techniques [42,68].

5.2. Magnetic Resonance Spectroscopy imaging (MRSi)

MRSi is a technique that uses spectroscopy but applies it to voxels across the entire brain. The concentration of the chemical of interest corresponds to the brightness or color of the voxel in the image produced. It can achieve high spatial resolution (up to 0.25 cm^3), and when optimized can produce a wealth of information [44,75]. This technique has largely been developed for breast cancer imaging, and can identify chemical "hot spots" that are of use when categorizing a tumor. It has great potential as a technique for understanding AD.

6. Concluding remarks

There is still a long way to go before AD can be fully understood and treated. With magnetic resonance technologies, it is possible to observe changes before cognitive decline begins. A lot of work has been done with structural imaging of gray and white matter, and changes are detectible in ApoE ε4 carriers decades before the onset of symptoms. More longitudinal studies need to be performed to determine which of these changes will specifically lead to AD. Functional studies offer a window of the changes that occur before neuronal atrophy, but the specific vascular causes behind the BOLD effect need to be further studied. Finally, chemical imaging can provide a glimpse of the changes occurring at the molecular level, and by further developing and standardizing these measures there is much that can be learned.

Author details

Emily J. Mason[1*], Manus J. Donahue[2] and Brandon A. Ally[1]

*Address all correspondence to: emily.mason.1@vanderbilt.edu

1 Department of Neurology, Vanderbilt University, Nashville, TN, USA

2 Department of Radiology, Vanderbilt University, Nashville, TN, USA

References

[1] Lind J, Persson J, Ingvar M, Larsson A, Cruts M, Van Broeckhoven C, et al. Reduced functional brain activity response in cognitively intact apolipoprotein E epsilon4 carriers. Brain. 2006 May;129(Pt 5):1240–8.

[2] Wilcock DM. The usefulness and challenges of transgenic mouse models in the study of Alzheimer's disease. CNS Neurol Disord Drug Targets. 2010 Aug.;9(4):386–94.

[3] Persson J, Lind J, Larsson A, Ingvar M, Sleegers K, Van Broeckhoven C, et al. Altered deactivation in individuals with genetic risk for Alzheimer's disease. Neuropsychologia. 2008;46(6):1679–87.

[4] Fleisher AS, Sherzai A, Taylor C, Langbaum JBS, Chen K, Buxton RB. Resting-state BOLD networks versus task-associated functional MRI for distinguishing Alzheimer's disease risk groups. NeuroImage. 2009 Oct. 1;47(4):1678–90.

[5] Sinha G. Peering inside Alzheimer's brains. Nat. Biotechnol. 2011 May;:384–7.

[6] Filippini N, Macintosh BJ, Hough MG, Goodwin GM, Frisoni GB, Smith SM, et al. Distinct patterns of brain activity in young carriers of the APOE-epsilon4 allele. Proc Natl Acad Sci USA. 2009 Apr. 28;106(17):7209–14.

[7] Boly M, Phillips C, Tshibanda L, Vanhaudenhuyse A, Schabus M, Dang-Vu TT, et al. Intrinsic brain activity in altered states of consciousness: how conscious is the default mode of brain function? Ann N Y Acad Sci. 2008;1129:119–29.

[8] Greicius MD, Srivastava G, Reiss AL, Menon V. Default-mode network activity distinguishes Alzheimer's disease from healthy aging: evidence from functional MRI. Proc Natl Acad Sci USA. 2004 Mar. 30;101(13):4637–42.

[9] Alzheimer's Association. 2012 Alzheimer's disease facts and figures. Alzheimers Dement. 8th ed. 2012 Mar. 5;:131–68.

[10] Plewes DB, Kucharczyk W. Physics of MRI: a primer. J Magn Reson Imaging. 2012 May;35(5):1038–54.

[11] Braak H, Braak E. Neuropathological stageing of Alzheimer-related changes. Acta Neuropathol. 1991;82(4):239–59.

[12] Jack CR Jr., Bernstein MA, Borowski BJ, Gunter JL, Fox NC, Thompson PM, et al. Update on the Magnetic Resonance Imaging core of the Alzheimer's Disease Neuroimaging Initiative. Alzheimer's and Dementia. 2010 May;6(3):212–20.

[13] Poels MMF, Ikram MA, van der Lugt A, Hofman A, Niessen WJ, Krestin GP, et al. Cerebral microbleeds are associated with worse cognitive function: the Rotterdam Scan Study. Neurology. 2012 Jan. 31;78(5):326–33.

[14] Pettersen JA, Sathiyamoorthy G, Gao F-Q, Szilagyi G, Nadkarni NK, St George-Hyslop P, et al. Microbleed topography, leukoaraiosis, and cognition in probable Alzheimer disease from the Sunnybrook dementia study. Arch Neurol. 2008 Jun.;65(6): 790–5.

[15] Cuingnet R, Gerardin E, Tessieras J, Auzias G, Lehéricy S, Habert M-O, et al. Automatic classification of patients with Alzheimer's disease from structural MRI: a comparison of ten methods using the ADNI database. NeuroImage. 2011 May 15;56(2): 766–81.

[16] Smith MA, Zhu X, Tabaton M, Liu G, McKeel DW, Cohen ML, et al. Increased iron and free radical generation in preclinical Alzheimer disease and mild cognitive impairment. J Alzheimers Dis. 2010;19(1):363–72.

[17] Chincarini A, Bosco P, Calvini P, Gemme G, Esposito M, Olivieri C, et al. Local MRI analysis approach in the diagnosis of early and prodromal Alzheimer's disease. NeuroImage. 2011 Sep. 15;58(2):469–80.

[18] Hopp K, Popescu BFG, McCrea RPE, Harder SL, Robinson CA, Haacke ME, et al. Brain iron detected by SWI high pass filtered phase calibrated with synchrotron X-ray fluorescence. J Magn Reson Imaging. 2010 Jun.;31(6):1346–54.

[19] Costafreda SG, Dinov ID, Tu Z, Shi Y, Liu C-Y, Kloszewska I, et al. Automated hippocampal shape analysis predicts the onset of dementia in mild cognitive impairment. NeuroImage. 2011 May 1;56(1):212–9.

[20] Ringman JM, Pope W, Salamon N. Insensitivity of visual assessment of hippocampal atrophy in familial Alzheimer's disease. J Neurol. 2010 May 1;257(5):839–42.

[21] Shaw P, Lerch JP, Pruessner JC, Taylor KN, Rose AB, Greenstein D, et al. Cortical morphology in children and adolescents with different apolipoprotein E gene polymorphisms: an observational study. Lancet Neurol. 2007 Jun. 1;6(6):494–500.

[22] Alexander GE, Bergfield KL, Chen K, Reiman EM, Hanson KD, Lin L, et al. Gray matter network associated with risk for Alzheimer's disease in young to middle-aged adults. Neurobiology of aging. 2012 Dec.;33(12):2723–32.

[23] Donix M, Burggren AC, Suthana NA, Siddarth P, Ekstrom AD, Krupa AK, et al. Family history of Alzheimer's disease and hippocampal structure in healthy people. Am J Psychiatry. 2010 Nov. 1;167(11):1399–406.

[24] Donix M, Burggren AC, Suthana NA, Siddarth P, Ekstrom AD, Krupa AK, et al. Longitudinal changes in medial temporal cortical thickness in normal subjects with the APOE-4 polymorphism. NeuroImage. 2010 Oct. 15;53(1):37–43.

[25] Espeseth T, Westlye LT, Fjell AM, Walhovd KB, Rootwelt H, Reinvang I. Accelerated age-related cortical thinning in healthy carriers of apolipoprotein E epsilon 4. Neurobiology of aging. 2008 Mar. 1;29(3):329–40.

[26] Grothe M, Heinsen H, Teipel SJ. Atrophy of the cholinergic Basal forebrain over the adult age range and in early stages of Alzheimer's disease. Biol Psychiatry. 2012 May 1;71(9):805–13.

[27] Brickman AM, Honig LS, Scarmeas N, Tatarina O, Sanders L, Albert MS, et al. Measuring cerebral atrophy and white matter hyperintensity burden to predict the rate of cognitive decline in Alzheimer disease. Arch Neurol. 2008 Sep.;65(9):1202–8.

[28] Yoshita M, Fletcher E, Harvey D, Ortega M, Martinez O, Mungas DM, et al. Extent and distribution of white matter hyperintensities in normal aging, MCI, and AD. Neurology. 2006 Dec. 26;67(12):2192–8.

[29] Carmichael O, Schwarz C, Drucker D, Fletcher E, Harvey D, Beckett L, et al. Longitudinal changes in white matter disease and cognition in the first year of the Alzheimer disease neuroimaging initiative. Arch Neurol. 2010 Nov.;67(11):1370–8.

[30] Sexton CE, Kalu UG, Filippini N, Mackay CE, Ebmeier KP. A meta-analysis of diffusion tensor imaging in mild cognitive impairment and Alzheimer's disease. Neurobiology of aging. 2011 Dec.;32(12):2322.e5–18.

[31] Smith EE, Egorova S, Blacker D, Killiany RJ, Muzikansky A, Dickerson BC, et al. Magnetic resonance imaging white matter hyperintensities and brain volume in the prediction of mild cognitive impairment and dementia. Arch Neurol. 2008 Jan.;65(1): 94–100.

[32] Appel J, Potter E, Bhatia N, Shen Q, Zhao W, Greig MT, et al. Association of white matter hyperintensity measurements on brain MR imaging with cognitive status, medial temporal atrophy, and cardiovascular risk factors. American Journal of Neuroradiology. 2009 Nov.;30(10):1870–6.

[33] Hirono N, Yasuda M, Tanimukai S, Kitagaki H, Mori E. Effect of the apolipoprotein E epsilon4 allele on white matter hyperintensities in dementia. Stroke. 2000 Jun.;31(6): 1263–8.

[34] Sawada H, Udaka F, Izumi Y, Nishinaka K, Kawakami H, Nakamura S, et al. Cerebral white matter lesions are not associated with apoE genotype but with age and female sex in Alzheimer's disease. J. Neurol. Neurosurg. Psychiatr. 2000 May;68(5): 653–6.

[35] Persson J, Lind J, Larsson A, Ingvar M, Cruts M, Van Broeckhoven C, et al. Altered brain white matter integrity in healthy carriers of the APOE epsilon4 allele: a risk for AD? Neurology. 2006 Apr. 11;66(7):1029–33.

[36] Høgh P, Garde E, Mortensen EL, Jørgensen OS, Krabbe K, Waldemar G. The apolipoprotein E epsilon4-allele and antihypertensive treatment are associated with in-

creased risk of cerebral MRI white matter hyperintensities. Acta Neurol. Scand. 2007 Apr.;115(4):248–53.

[37] Ryan L, Walther K, Bendlin BB, Lue L-F, Walker DG, Glisky EL. Age-related differences in white matter integrity and cognitive function are related to APOE status. NeuroImage. 2011 Jan. 15;54(2):1565–77.

[38] Bendlin BB, Ries ML, Canu E, Sodhi A, Lazar M, Alexander AL, et al. White matter is altered with parental family history of Alzheimer's disease. Alzheimers Dement. 2010 Sep. 1;6(5):394–403.

[39] Smith CD, Chebrolu H, Andersen AH, Powell DA, Lovell MA, Xiong S, et al. White matter diffusion alterations in normal women at risk of Alzheimer's disease. Neurobiology of aging. 2010 Jul. 1;31(7):1122–31.

[40] Atwood CS, Obrenovich ME, Liu T, Chan H, Perry G, Smith MA, et al. Amyloid-beta: a chameleon walking in two worlds: a review of the trophic and toxic properties of amyloid-beta. Brain Res. Brain Res. Rev. 2003 Sep.;43(1):1–16.

[41] Brewer JB, Magda S, Airriess C, Smith ME. Fully-automated quantification of regional brain volumes for improved detection of focal atrophy in Alzheimer disease. American Journal of Neuroradiology. 2009 Mar. p. 578–80.

[42] la Torre de JC. Is Alzheimer's disease a neurodegenerative or a vascular disorder? Data, dogma, and dialectics. Lancet Neurol. 2004 Mar. 1;3(3):184–90.

[43] Sperling R. Functional MRI Studies of Associative Encoding in Normal Aging, Mild Cognitive Impairment, and Alzheimer's Disease. Ann N Y Acad Sci. 2007 Feb. 1;1097(1):146–55.

[44] Trachtenberg AJ, Filippini N, Mackay CE. The effects of APOE-ε4 on the BOLD response. NBA. Elsevier Inc; 2012 Feb. 1;33(2):323–34.

[45] Sugarman MA, Woodard JL, Nielson KA, Seidenberg M, Smith JC, Durgerian S, et al. Functional magnetic resonance imaging of semantic memory as a presymptomatic biomarker of Alzheimer's disease risk. Biochimica et Biophysica Acta (BBA) - Molecular Basis of Disease. 2012 Mar.;1822(3):442–56.

[46] Seidenberg M, Guidotti L, Nielson KA, Woodard JL, Durgerian S, Antuono P, et al. Semantic memory activation in individuals at risk for developing Alzheimer disease. Neurology. 2009 Aug. 25;73(8):612–20.

[47] Woodard JL, Seidenberg M, Nielson KA, Antuono P, Guidotti L, Durgerian S, et al. Semantic memory activation in amnestic mild cognitive impairment. Brain. 2009 Aug.;132(Pt 8):2068–78.

[48] Sorg C, Riedl V, Muhlau M, Calhoun VD, Eichele T, Laer L, et al. Selective changes of resting-state networks in individuals at risk for Alzheimer's disease. Proc Natl Acad Sci USA. 2007 Nov. 20;104(47):18760–5.

[49] Luchtmann M, Jachau K, Tempelmann C, Bernarding J. Alcohol induced region-dependent alterations of hemodynamic response: implications for the statistical interpretation of pharmacological fMRI studies. Exp Brain Res. 2010 Jul.;204(1):1–10.

[50] Koppelstaetter F, Poeppel TD, Siedentopf CM, Ischebeck A, Kolbitsch C, Mottaghy FM, et al. Caffeine and cognition in functional magnetic resonance imaging. J Alzheimers Dis. 2010;20 Suppl 1:S71–84.

[51] Donahue MJ, Blicher JU, Østergaard L, Feinberg DA, Macintosh BJ, Miller KL, et al. Cerebral blood flow, blood volume, and oxygen metabolism dynamics in human visual and motor cortex as measured by whole-brain multi-modal magnetic resonance imaging. J Cereb Blood Flow Metab. 2009 Nov.;29(11):1856–66.

[52] KETY SS, SCHMIDT CF. The nitrous oxide method for the quantitative determination of cerebral blood flow in man; theory, procedure and normal values. J. Clin. Invest. 1948 Jul.;27(4):476–83.

[53] Corder EH, Saunders AM, Strittmatter WJ, Schmechel DE, Gaskell PC, Small GW, et al. Gene dose of apolipoprotein E type 4 allele and the risk of Alzheimer's disease in late onset families. Science. 1993 Aug. 13;261(5123):921–3.

[54] Ishii K, Sasaki M, Yamaji S, Sakamoto S, Kitagaki H, Mori E. Demonstration of decreased posterior cingulate perfusion in mild Alzheimer's disease by means of H215O positron emission tomography. Eur J Nucl Med. 1997 Jun.;24(6):670–3.

[55] Bartenstein P, Minoshima S, Hirsch C, Buch K, Willoch F, Mösch D, et al. Quantitative assessment of cerebral blood flow in patients with Alzheimer's disease by SPECT. J. Nucl. Med. 1997 Jul.;38(7):1095–101.

[56] Kogure D, Matsuda H, Ohnishi T, Asada T, Uno M, Kunihiro T, et al. Longitudinal evaluation of early Alzheimer's disease using brain perfusion SPECT. J. Nucl. Med. 2000 Jul.;41(7):1155–62.

[57] Schmitz BL, Aschoff AJ, Hoffmann MHK, Grön G. Advantages and pitfalls in 3T MR brain imaging: a pictorial review. AJNR Am J Neuroradiol. 2005 Oct.;26(9):2229–37.

[58] Alsop DC, Detre JA, Grossman M. Assessment of cerebral blood flow in Alzheimer's disease by spin-labeled magnetic resonance imaging. Ann Neurol. 2000 Jan.;47(1):93–100.

[59] Johnson NA, Jahng G-H, Weiner MW, Miller BL, Chui HC, Jagust WJ, et al. Pattern of cerebral hypoperfusion in Alzheimer disease and mild cognitive impairment measured with arterial spin-labeling MR imaging: initial experience. Radiology. 2005 Mar.;234(3):851–9.

[60] Kim SM, Kim MJ, Rhee HY, Ryu C-W, Kim EJ, Petersen ET, et al. Regional cerebral perfusion in patients with Alzheimer's disease and mild cognitive impairment: effect of APOE Epsilon4 allele. Neuroradiology. 2012 Jul. 25.

[61] Uh J, Lewis-Amezcua K, Martin-Cook K, Cheng Y, Weiner M, Diaz-Arrastia R, et al. Cerebral blood volume in Alzheimer's disease and correlation with tissue structural integrity. Neurobiology of aging. 2010 Dec.;31(12):2038–46.

[62] Vernooij MD M, Smits MD M. Structural Neuroimaging in Aging and Alzheimer's Disease. Neuroimaging Clinics of NA. Elsevier Inc; 2012 Feb. 1;22(1):33–55.

[63] Lu H, Law M, Johnson G, Ge Y, Van Zijl PCM, Helpern JA. Novel approach to the measurement of absolute cerebral blood volume using vascular-space-occupancy magnetic resonance imaging. Magn Reson Med. 2005 Dec. 1;54(6):1403–11.

[64] Grubb RL, Raichle ME, Eichling JO, Ter-Pogossian MM. The effects of changes in PaCO2 on cerebral blood volume, blood flow, and vascular mean transit time. Stroke. 1974 Sep.;5(5):630–9.

[65] Donahue MJ, Strother MK, Hendrikse J. Novel MRI approaches for assessing cerebral hemodynamics in ischemic cerebrovascular disease. Stroke. 2012 Mar.;43(3):903–15.

[66] Kantarci K. 1H magnetic resonance spectroscopy in dementia. Br J Radiol. 2007 Dec.; 80 Spec No 2:S146–52.

[67] Kantarci K, Smith GE, Ivnik RJ, Petersen RC, Boeve BF, Knopman DS, et al. 1H magnetic resonance spectroscopy, cognitive function, and apolipoprotein E genotype in normal aging, mild cognitive impairment and Alzheimer's disease. J Int Neuropsychol Soc. 2002 Nov.;8(7):934–42.

[68] Schott JM, Frost C, Macmanus DG, Ibrahim F, Waldman AD, Fox NC. Short echo time proton magnetic resonance spectroscopy in Alzheimer's disease: a longitudinal multiple time point study. Brain. 2010 Nov. 1;133(11):3315–22.

[69] Selkoe DJ. Alzheimer's disease is a synaptic failure. Science. 2002 Oct. 25;298(5594): 789–91.

[70] Limon A, Reyes-Ruiz JM, Miledi R. Loss of functional GABAA receptors in the Alzheimer diseased brain. Proc Natl Acad Sci USA. 2012 Jun. 19;109(25):10071–6.

[71] Waddell KW, Avison MJ, Joers JM, Gore JC. A practical guide to robust detection of GABA in human brain by J-difference spectroscopy at 3 T using a standard volume coil. Magn Reson Imaging. 2007 Sep.;25(7):1032–8.

[72] Zhang H, Wang W, Gao W, Ge Y, Zhang J, Wu S, et al. Effect of propofol on the levels of neurotransmitters in normal human brain: A magnetic resonance spectroscopy study. Neurosci Lett. 2009 Dec.;467(3):247–51.

[73] Harada M, Kubo H, Nose A, Nishitani H, Matsuda T. Measurement of variation in the human cerebral GABA level by in vivo MEGA-editing proton MR spectroscopy using a clinical 3 T instrument and its dependence on brain region and the female menstrual cycle. Hum. Brain Mapp. 2011 May;32(5):828–33.

http://dx.doi.org/10.5772/54445

[74] Falini A, Bozzali M, Magnani G, Pero G, Gambini A, Benedetti B, et al. A whole brain MR spectroscopy study from patients with Alzheimer's disease and mild cognitive impairment. NeuroImage. 2005 Jul. 15;26(4):1159–63.

[75] Hu J, Feng W, Hua J, Jiang Q, Xuan Y, Li T, et al. A high spatial resolution in vivo 1H magnetic resonance spectroscopic imaging technique for the human breast at 3 T. Med Phys. 2009 Nov.;36(11):4870–7.